


# One-pot synthesis of anilides, herbicidal activity and molecular docking study

Suélien K Sartori,<sup>a</sup> Elson S Alvarenga,<sup>a\*</sup>  Cristiane A Franco,<sup>a</sup> Danielle S Ramos<sup>a</sup> and Denilson F Oliveira<sup>b</sup>



## Abstract

**BACKGROUND:** In the context of the demand for more efficient herbicides, the aim of the present work was to synthesize anilides via simple methods, and evaluate their herbicidal activities through seed germination assays. *In silico* studies were carried out to identify the enzyme target sites in plants for the most active anilides.

**RESULTS:** A total of 18 anilides were prepared via one-pot reaction in yields that varied from 36 to 98% through reactions of anilines with sorbic chloride and hexanoic anhydride. According to seed germination assays in three dicotyledonous and one monocotyledonous plant species, the most active anilides showed root and shoot growth inhibition superior to that of Dual (*S*-metolachlor). *In silico* studies indicated that histone deacetylase was the probable enzyme target site in plants for these substances. The affinities of the most active anilides for the binding sites of this enzyme were equal to or higher than those calculated for its inhibitors.

**CONCLUSION:** Anilides 4d, 4e, 4g, and 4h are promising candidates for the development of novel herbicides. According to *in silico* studies, they inhibit histone deacetylase in plants, which can be exploited for the development of new weed control methods.

© 2018 Society of Chemical Industry

Supporting information may be found in the online version of this article.

**Keywords:** lettuce; beggartick; cucumber; onion; computational study

## 1 INTRODUCTION

About 30 to 40% of losses in food production are attributable to the presence of weeds in crops.<sup>1</sup> In melon (*Cucumis melo* L.), for example, losses can reach 100%.<sup>2</sup> In such cases, it is necessary to use agrochemicals to control these pests. This situation is very often observed in countries such as Brazil, which was the ninth largest producer of melons worldwide in 2012.<sup>3</sup> In addition, Brazil is currently the second largest agricultural exporter and the largest supplier of sugar, orange juice and coffee in the world. In 2013, it reached the position of the largest soybean supplier in the world, surpassing the USA, and in that year 36% of total Brazilian exports were related to agribusiness. It is thus essential to carry out research with the aim of obtaining new herbicides for use in this industry in Brazil.<sup>4</sup>

Anilides are a class of amides that have been extensively studied because of their various biological activities, such as antimycobacterial,<sup>5,6</sup> antifungal,<sup>7</sup> larvicidal,<sup>8</sup> tuberculostatic,<sup>9</sup> insecticidal<sup>10</sup> and herbicidal activities.<sup>11</sup> In addition, some anilides such as acetanilide, acetaminophen [*N*-(4-hydroxyphenyl)acetamide], and phenacetin [*N*-(4-ethoxyphenyl)ethanamide] are employed in the pharmaceutical industry as antipyretic analgesics.<sup>12</sup>

Currently, many anilides are used as herbicides in agriculture, as they are easily obtained by reactions of aromatic amines with acyl chlorides or with carboxylic acid anhydrides, known as 'one-pot' reactions.<sup>13</sup> For example, propanil [*N*-(3,4-dichlorophenyl)propanamide], which belongs to the acetanilide

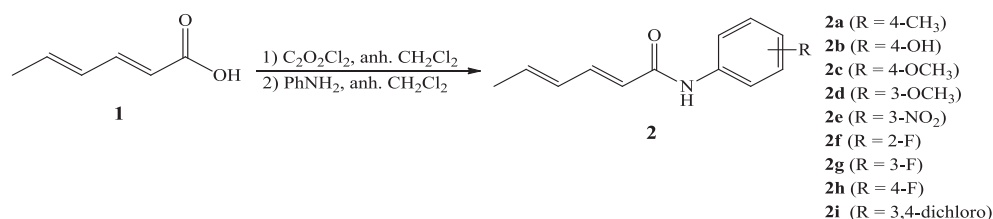
class, is used as a post-emergent herbicide for the control of grasses and broadleaf weeds mainly in rice (*Oryza sativa* L.) plantations<sup>14</sup>; butachlor [*N*-(butoxymethyl)-2-chloro-*N*-(2,6-diethylphenyl)acetamide], belonging to the class of chloroacetanilides, is a pre-emergent herbicide used in the control of several annual grasses<sup>15</sup>; alachlor [2-chloro-2',6'-diethyl-*N*-(methoxymethyl)acetanilide], also a representative of the class of chloroacetanilides, is employed as a pre- and post-emergent herbicide in corn, soybean and peanut plantations for the control of several weeds<sup>16</sup>; *S*-metolachlor [(*S*)-2-chloro-*N*-(2-ethyl-6-methylphenyl)-*N*-(1-methoxypropan-2-yl)acetamide], another example of the class of chloroacetanilides, is a selective pre-emergent herbicide used to control weeds in soybean, corn, sugarcane, bean and cotton crops.<sup>17</sup>

Many of the herbicides used in crop protection act as photosynthesis inhibitors; for example, acetanilides. One such inhibitor is propanil, which was discovered by Rohm and Haas in 1957 and has its effect by interrupting the electron transport chain through inhibition of photosystem II, which consequently inhibits plant growth.<sup>14</sup> In addition to this herbicide, Miletin

\* Correspondence to: ES Alvarenga, Chemistry Department, Universidade Federal de Viçosa, Viçosa, MG, Brazil. E-mail: elson@ufv.br

a Chemistry Department, Universidade Federal de Viçosa, Viçosa, MG, Brazil

b Chemistry Department, Universidade Federal de Lavras, Lavras, MG, Brazil



**Scheme 1.** Synthesis of the amides **2a–i**.

*et al.*<sup>18</sup> reported the synthesis of a series of anilides derived from 2-alkylpyridine-4-carboxylic acid that inhibited the photosynthetic electron transport chain in spinach chloroplasts. The site of their action is the  $Z^+/D^+$  intermediate, or tyrosine radicals, which are located on the  $D_1$  and  $D_2$  proteins on the donor side of photosystem II.<sup>11</sup> This was confirmed by Král'ová *et al.*<sup>11,19</sup> by the use of the electronic spin resonance (ESR) spectroscopy technique.

Chloroacetanilides, in contrast, inhibit long-chain fatty acid (LCFA) biosynthesis, i.e., cell division and protein synthesis. Chloroacetanilides cause the death of plants that are susceptible to this mechanism of action.<sup>20</sup>

The process for the development of new bioactive compounds can be time-consuming and expensive. Therefore, several research groups are using computational chemistry, which can act as a virtual shortcut, speeding up the process and reducing the cost of research and development.<sup>21</sup> Several *in silico* methods have been used for this purpose, among which are docking and pharmacophore methods, which reveal interactions between organic compounds and enzymes.<sup>22</sup> For example, combined *in silico* structure-based pharmacophore and molecular docking-based virtual screening was used to identify novel herbicides that act through inhibition of *para*-hydroxyphenylpyruvate dioxygenase.<sup>23</sup>

In this context, we prepared 18 anilides via a 'one-pot reaction' to be screened against seeds of *Allium cepa* L., *Bidens pilosa* L., *Cucumis sativus* L., and *Lactuca sativa* L. The most active compounds then underwent computational studies to determine their enzyme target in plants.

## 2 MATERIALS AND METHODS

### 2.1 Chemicals

#### 2.1.1 General

The progress of the reactions was monitored by visualization of thin-layer chromatography (TLC) plates in an ultraviolet irradiation chamber with a 254 nm lamp.<sup>24</sup> All compounds were purified by column chromatography on silica gel (60–230 mesh; Sigma Aldrich, St. Louis, MO, USA) and, in some cases, the recrystallization technique was also employed. Melting points were obtained in a MQAPF-301 (Microquímica Equipamentos Ltda, Palhoça, Brazil) melting point apparatus and were not corrected. Infrared (IR) spectra were acquired using a Varian 660-IR spectrophotometer (equipped with GLADI-ATR, Agilent, Santa Clara, CA, USA) with the attenuated total reflectance (ATR) method. Nuclear magnetic resonance (NMR) spectra were recorded on a Varian Mercury 300-MHz spectrometer using  $CDCl_3$  and  $DMSO-d_6$  as solvents. The  $^1H$  NMR chemical shifts were reported using the residual signals of  $CHCl_3$  ( $\delta = 7.27$  ppm) and  $DMSO-d_5$  ( $\delta = 2.50$  ppm) as references.  $^{13}C$  NMR chemical shifts were recorded using the  $CDCl_3$  signal ( $\delta = 77.0$  ppm) and the  $DMSO-d_6$  signal ( $\delta = 39.5$  ppm) as references. The mass spectra were obtained on Shimadzu (Kyoto, Japan) GC–MS–QP5050A and GC–MS–QP2010 Ultra equipment after 70-eV electron impact ionization (EI). The  $^1H$  NMR and  $^{13}C$

NMR spectra of the anilides can be found in the Supporting Information.

#### 2.1.2 General procedure 1: synthesis of anilides **2a–i**

Sorbic acid (**1**; 0.500 g; 4.46 mmol), anhydrous dichloromethane (10.0 mL), and oxalyl chloride ( $C_2O_2Cl_2$ ) (1.0 mL; 11.15 mmol) were added to a two-neck round-bottomed flask and maintained under nitrogen atmosphere. The reaction mixture was stirred for 30 min and concentrated under vacuum. The residue (yellow oil) was dissolved in anhydrous dichloromethane (10.0 mL), and cooled in an ice bath (0 °C). The anilines (11.15 mmol) were added to the round-bottomed flask, and the mixture stirred for 2 h.

The solvent was removed under reduced pressure, and the residue purified by silica gel column chromatography to produce anilides **2a–i** (Scheme 1). The eluent employed in the column chromatography purification was a mixture of hexane and ethyl acetate. The proportion of hexane and ethyl acetate is inherent to each anilide, and is described in the Supplementary Information. Some of the products were further purified by recrystallization.

The spectra and spectrometric data for compounds **2a–i** can be found in the Supporting Information.

#### 2.1.3 General procedure 2: synthesis of anilides **4a–i**

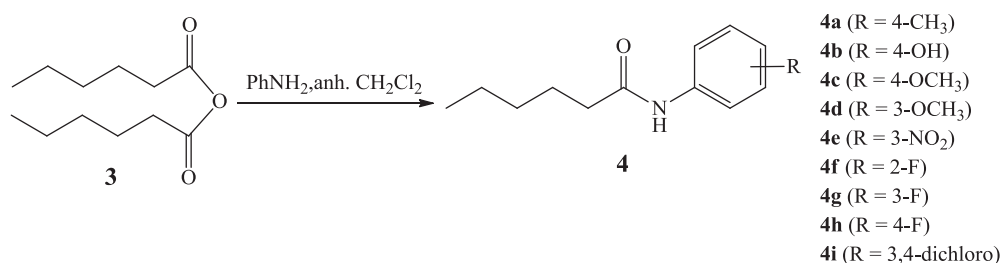
The anilines (2.45 mmol) were added to a solution of hexanoic anhydride 97% (v/v) (560  $\mu$ L; 2.35 mmol) in anhydrous dichloromethane (10.0 mL). The reaction mixture was stirred under nitrogen atmosphere for 2 h, and quenched with a saturated solution of sodium bicarbonate (20.0 mL). The organic phase was separated in a separating funnel and the aqueous phase was extracted with three portions of dichloromethane (20.0 mL). The combined organic phases were washed with 10 mL of 1 M HCl and dried over anhydrous sodium sulfate. The mixture was filtered and the solvent was evaporated under reduced pressure. The residue was purified by silica gel flash column chromatography to produce anilides **4a–i** (Scheme 2). The eluent employed in the column chromatography purification was a mixture of hexane and ethyl acetate. The proportion of hexane and ethyl acetate is inherent to each anilide, and is described in the Supporting Information. Some of the products were further purified by recrystallization.

The spectra and spectrometric data for compounds **4a–i** can be found in the Supporting Information.

## 2.2 Herbicidal bioassays

### 2.2.1 General procedures

The pre-emergent herbicidal activities of compounds **2a–i** and **4a–i** were evaluated against seeds of onion (*A. cepa* 'Texas Early Grano 502 PRR'), beggartick (*B. pilosa*), cucumber (*C. sativus* 'hick'), and lettuce (*L. sativa* 'Vitória Santo Antão'). The beggartick seeds employed in this study were collected in November 2015 at the Santa Juliana site, located in the rural area of Visconde do Rio Branco, Minas Gerais, Brazil (altitude 351 m; 20°59'25.55" S,



**Scheme 2.** Synthesis of the amides **4a–i**.

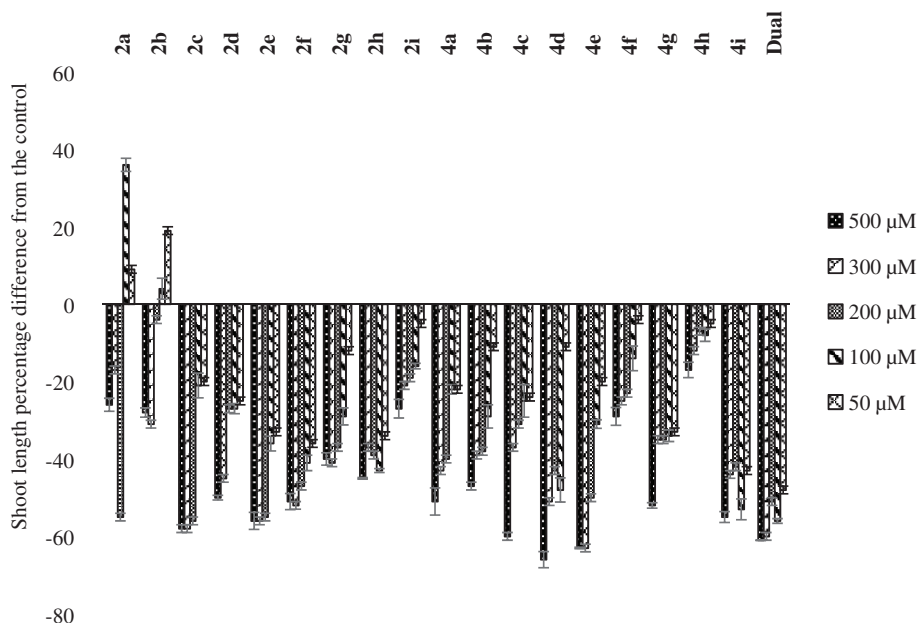


**Figure 1.** Effects of the compounds on shoot development of *A. cepa* relative to the control solution. Values are expressed as percentage difference from the control. The error bars represent the standard deviation.

42°48'11.88" W; coordinates obtained from the Google Earth application). In 90-mm-diameter Petri dishes containing germination paper, 20 onion seeds, 20 lettuce seeds, and 50 beggartick seeds were distributed and 5.0 ml of the test solution was added to each plate. A total of 20 seeds of cucumber and 9.0 mL of the test solution were added to 145-mm-diameter Petri dishes.<sup>25</sup> The dishes were sealed with plastic film and kept in a germination chamber (B.O.D., Piracicaba, Brazil) at 25 °C, in the absence of light, for 120 h (5 days).

The experiments were carried out in triplicate with test solutions at concentrations of 500, 300, 200, 100 and 50 μM. The solutions were prepared using 0.3% (v/v) aqueous dimethylsulfoxide (DMSO) solution. An aqueous solution of DMSO at 0.3% (v/v) and an aqueous solution of the commercial herbicide Dual (Dual Gold Syngenta® Company, São Paulo, Brazil; *S*-metolachlor) were used as negative and positive controls, respectively. After the growth period, the plates were frozen at 0 °C for 24 h (to facilitate handling of the seedlings in the next stage). The plates were removed from the freezer, and after 10 min the seeds were laid on black paper. The seeds were photographed with a digital camera and the lengths of shoots and roots measured with the aid of a computer program. The growth percentage of shoots and roots was calculated according to the following equation:

$$G(\%) = \frac{(S - C)}{C} 100$$

where *S* is the average length of the germinating shoots or roots of the plants, and *C* corresponds to the average growth of the negative control.<sup>26</sup>

## 2.3 Computational study

### 2.3.1 Conformational search for active anilides

The three-dimensional chemical structures of compounds **4d**, **4e**, **4g**, **4h**, and **4i**, which were the most active molecules in the experiments described above, were drawn using the program ChemSketch 12.01 (Advanced Chemistry Development, Inc., Toronto, Canada). The structures of compounds **4d**, **4e**, **4g**, **4h**, and **4i** were subjected to conformational searches with the Open3Dalign 2.8.2 software,<sup>27</sup> which considered water implicitly by using the Generalized Born Surface Area (GBSA) model. For each substance, the most stable conformation was selected, as well as all those up to 10 kcal mol<sup>-1</sup> distant from the most stable conformation, to be subjected to optimizations with the MOPAC 2012 computer program,<sup>28</sup> using the Hamiltonian PM7. In this case, water was implicitly considered by the use of the Conductor-like Model (COSMO). After calculating the Boltzmann distributions of the conformations of each substance, based on their total energies, the structures corresponding to at least 2% of the total were selected. These were observed in the VMD 1.9.2 computer program.<sup>29</sup> When a pair of similar conformations was observed, one of them was discarded.

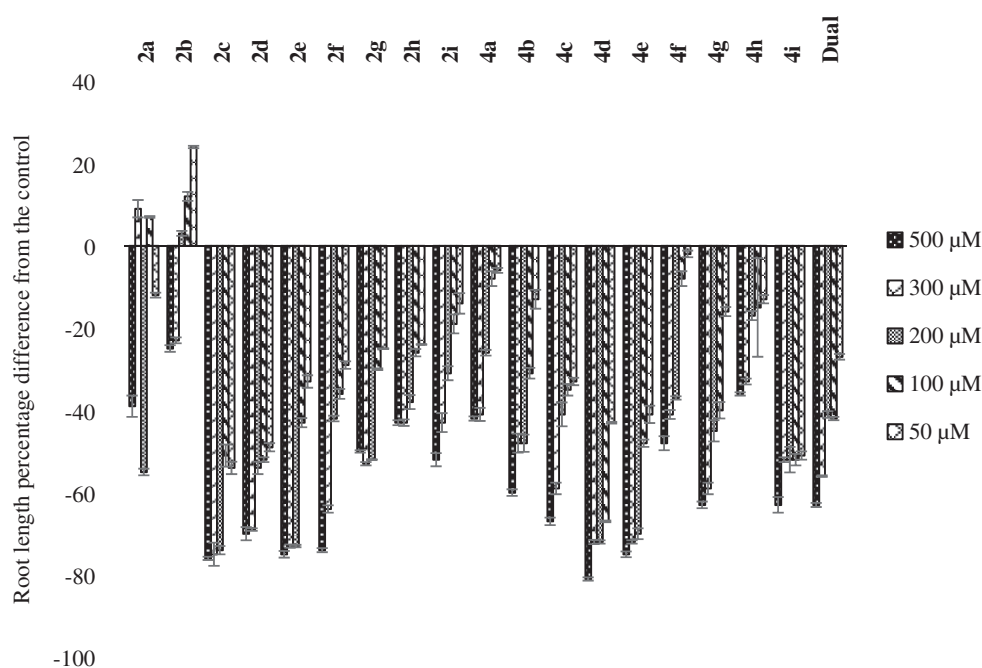


**Figure 2.** Effects of the compounds on root development of *A. cepa* relative to the control solution. Values are expressed as percentage difference from the control. The error bars represent the standard deviation.

### 2.3.2 Pharmacophoric search

The database of protein ligands Ligand Expo (<http://ligand-expo.rcsb.org>),<sup>30</sup> obtained through the RCSB Protein Data Bank (<http://www.pdb.org>),<sup>31</sup> was subjected to hydrogen addition using the OpenBabel 2.3.2 program,<sup>32</sup> to be compared to the selected conformations of compounds **4d**, **4e**, **4g**, **4h** and **4i** using the Align\_it 1.0.4 program,<sup>33</sup> which employed standard values for the various parameters. Only results with a Tanimoto score  $\geq 0.7$ <sup>34</sup> were selected for the next step: 1S6R,<sup>35</sup> 1V3V,<sup>36</sup> 2GH6,<sup>37</sup> 3AOU,<sup>38</sup> 4C4X,<sup>39</sup> and 5F1J.<sup>40</sup>

### 2.3.3 Search for amino acid sequences in the genomes of plants

The amino acid sequences of the enzymes selected through the pharmacophoric search (1S6R, 1V3V, 2GH6, 3AOU, 4C4X and 5F1J) were downloaded from the Research Collaboratory for Structural Bioinformatics (RCSB) Protein Data Bank (<http://www.pdb.org>),<sup>31</sup> to be used in searches for similar sequences in the genomes of plants through the National Center for Biotechnology Information (NCBI; <http://www.ncbi.nlm.nih.gov>). The program Blastp 2.3.1+<sup>41,42</sup> was employed with the Domain Enhanced Lookup Time Accelerated BLAST (Delta-BLAST) algorithm<sup>43</sup> set to the default parameters. This search was carried out in all non-redundant (nr) database, which is much bigger returning a much closer match. The enzyme with the highest scores was selected for the next step.

### 2.3.4 Selection of histone deacetylases

The amino acid sequences of all histone deacetylase enzymes in the RCSB Protein Data Bank<sup>31</sup> were downloaded and compared using the Ugene1.16.2 program<sup>44</sup> and the ClustalO 1.2.1 algorithm<sup>45</sup> with 10 iterations. All enzymes with <90% similarity to 2GH6 (number of amino acid residues = 369) and/or with numbers of amino acid residues outside the  $369 \pm 60$  range were eliminated. Then, the three-dimensional structures of the selected enzymes were observed in the VMD 1.9.2 computer program,<sup>29</sup> which allowed us to verify that several of them had

missing amino acid residues in their active sites or near them, which led to the elimination of such structures. Those that were mutants were also eliminated. The pdb files of the remaining enzymes were submitted to the Python Makemultimer script (<http://watcut.uwaterloo.ca/makemultimer/index>) to obtain the corresponding three-dimensional monomeric structures, which were aligned with the use of the Lovoalign 1.1.0 program.<sup>46</sup> The three-dimensional structures of the selected histone deacetylases above were submitted to the Autopsf plugin of the VMD 1.9.2 software<sup>29</sup> for the addition of missing atoms in such structures. Then, using Autodock Tools 1.5.7rc1,<sup>47</sup> the pdb files were converted to pdbqt format.

### 2.3.5 Docking

The three-dimensional chemical structures of 9,9,9-trifluoro-8-oxo-*N*-phenylnonanamide (CF3),<sup>37</sup> *N*-(4-aminobiphenyl-3-yl) benzamide (LLX),<sup>48</sup> 4-(dimethylamino)-*N*-[7-(hydroxyamino)-7-oxoheptyl]benzamide (B3N),<sup>49</sup> (2*R*)-2-amino-3-(3-chlorophenyl)-1-[4-(2,5-difluorobenzoyl)piperazin-1-yl]propan-1-one (ODI),<sup>50</sup> and methyl 4-bromo-*N*-[8-(hydroxyamino)-8-oxooctanoyl]-L-phenylalaninate (S17),<sup>51</sup> which are inhibitors of histone deacetylases, were drawn and subjected to conformational searches as described above. The pdb files of the most stable conformations of such substances, as well as of anilides **4d**, **4e**, **4g**, **4h**, and **4i**, after optimization with MOPAC 2012, were converted to the pdbqt format using AutodockTools 1.5.7rc1.<sup>47</sup> Then the program Autogrid 4.2.6<sup>47</sup> was used for calculations of atomic affinities in parallelepipedal regions ( $26.25 \times 26.25 \times 26.25 \text{ \AA}^3$ ) centered on the CF3 molecules found in active sites of the enzyme present in the 2GH6 complex.<sup>37</sup> The Autodock 4.2.6 program<sup>47</sup> used such affinities to dock the above-mentioned substances to the enzyme sites. With the exception of the ga\_num\_evals\_parameter, which was raised from 2500000 to 5000000, the other parameters were kept at the default values of the program. Finally, the values obtained with the software Autodock<sup>47</sup> were subjected to analysis



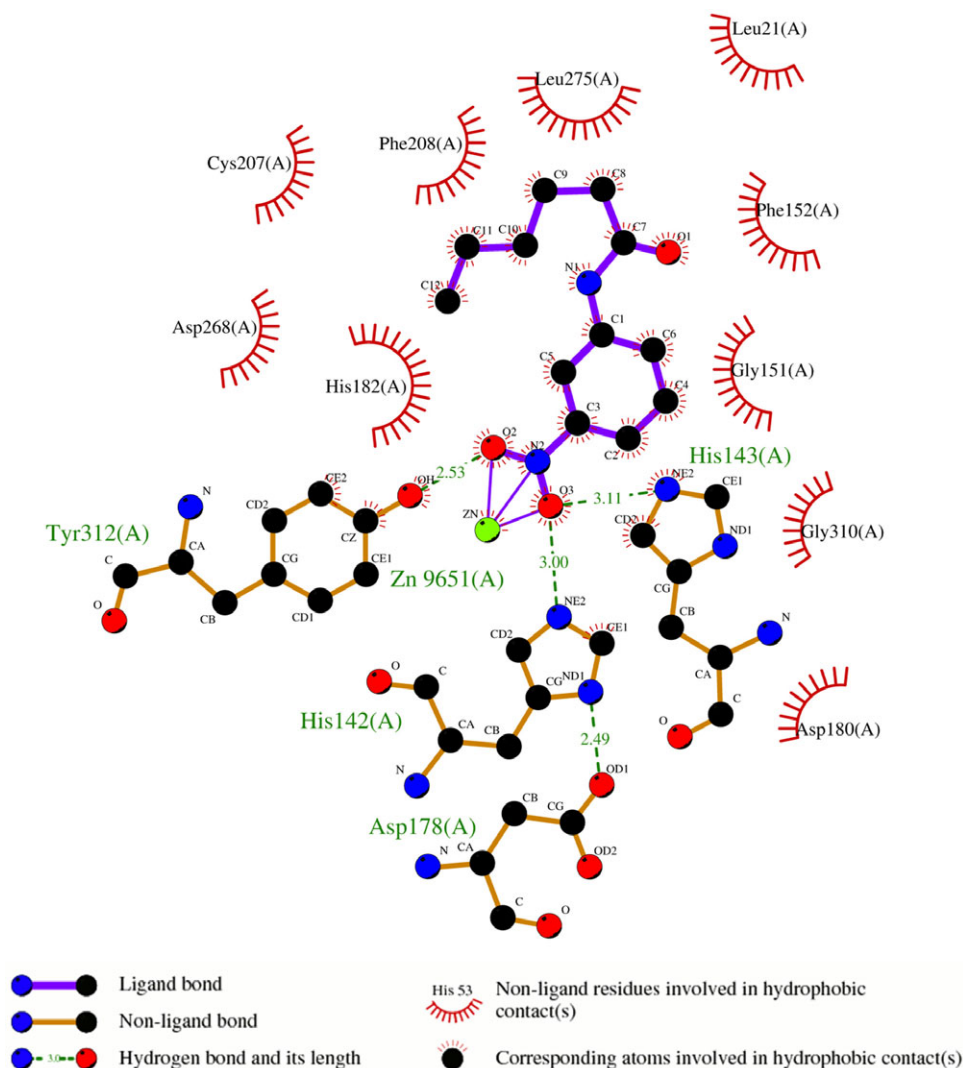


**Figure 3.** Two-dimensional representation of the interaction of *N*-(3-nitrophenyl)hexanamide (**4e**) with the enzyme histone deacetylase from *Alcaligenaceae bacterium* (code 1GH6 in the Protein Data Bank; <http://www.pdb.org>). The ligand was docked to the active site of the enzyme with the software Autodock 4.2.6.<sup>47</sup> The image was generated in the software LigProt+1.4.5.<sup>60</sup>

of variance (ANOVA), followed by means comparison according to the Scott and Knott test ( $P \leq 0.05$ ). For this, the Sisvar computer program<sup>52</sup> was used.

### 3 RESULTS AND DISCUSSION

#### 3.1 Chemical synthesis

The anilides **2a–i** were prepared from sorbic acid via reaction with oxalyl chloride to prepare to acid chloride. The reactive acid chloride was quenched with nine distinct anilines to obtain the desired anilides **2a–i**. These amides were purified by silica gel flash column chromatography and some of them were even recrystallized. These anilides were fully characterized by spectrometric methods.

The one-pot reaction was the approach used to prepare anilides **4a–i**, where the anilines were combined with hexanoic anhydride in DCM to provide a total of nine hexanamides. Anilides **4a–i** were purified and fully characterized by infrared spectrophotometry, <sup>1</sup>H NMR, <sup>13</sup>C NMR, and mass spectrometry. All physical properties and spectrometric data for compounds **2a–i** and **4a–i** can be found in the Supporting Information.

#### 3.2 Herbicidal activity

##### 3.2.1 Activity against *Allium cepa*, a monocotyledonous plant (Figs 1 and 2)

All anilides inhibited shoot growth, with **4d** and **4e** being the most active compounds, inhibiting growth by 66 and 63%, respectively. This effect reached a maximum at 500  $\mu\text{M}$ , and then decreased with increasing concentration. Compounds **2c**, **2d**, **2e**, **2f**, **4d**, and **4e** inhibited the growth of roots at a concentration of 500  $\mu\text{M}$  by 76, 69, 75, 74, 81, and 75%, respectively, while the commercial herbicide Dual Gold inhibited growth by 63%.

##### 3.2.2 Activity against *Lactuca sativa*, a dicotyledonous plant (Figs S1 and S2 in Supporting Information)

Compounds **2e**, **4d**, **4e**, and **4g** inhibited the growth of the shoot at 500  $\mu\text{M}$  by 71, 64, 68, and 61%, respectively. At this concentration, anilide **2e** showed 7% greater inhibition of the aerial parts than that obtained with Dual.

The commercial herbicide inhibited the growth of the roots by 26% at 500  $\mu\text{M}$ , while anilides **2d**, **2e**, **4d**, and **4e** inhibited growth by 64, 64, 67, and 64%, respectively.

In addition, compounds **2i**, **4a**, **4c**, and **4i** showed inhibition of the roots of >50% at this concentration. However, anilide **2f** stimulated development of the roots by >50% at concentrations of 300, 200, 100, and 50  $\mu\text{M}$ . For the monocotyledonous plant *A. cepa*, **2f** showed high inhibitory activity. The most active anilides **2e**, **4d**, **4e**, and **4g** have in common a substituent on the aromatic ring at the *meta* position.

### 3.2.3 Activity against *Cucumis sativus*, a dicotyledonous plant (Figs S3 and S4 in Supporting Information)

The most active compounds **4d**, **4e**, and **4h** showed percentages of shoot growth inhibition of 60, 74, and 65% at 500  $\mu\text{M}$ , respectively. The radicular part of this plant was inhibited by 77, 78, 71, and 77% by **4d**, **4e**, **4g**, and **4h**, respectively. In general, these compounds caused greater inhibition at the concentration of 500  $\mu\text{M}$  for both roots and shoots of this plant than Dual.

### 3.2.4 *Bidens pilosa*, a dicotyledonous plant (Figs S5 and S6 in Supporting Information)

The highest percentage of inhibition of the shoots of the seedlings was obtained for the anilides **4e** and **2b**. Compounds **4e** and **2b** hindered growth of the shoot by 81 and 72%, respectively. The growth of roots was also strongly inhibited by these two compounds, indicating that they are candidate herbicides against the weed beggartick. Another interesting finding is that compound **2b** inhibited growth of both the aerial parts and roots of *B. pilosa*, while acting as a growth stimulator for the other plants. This is an interesting finding as it suggests that **2b** could be used as a selective herbicide for *B. pilosa* without inhibiting other crops.

## 3.3 Computational study

In order to identify the enzymatic target of the phytotoxic amides, a pharmacophoric search was carried out with the most stable conformations of anilides **4d**, **4e**, **4g**, **4h** and **4i**, which were the most active in the experiments carried out in the present work. This resulted in the selection of six enzymes, 1S6R, 1V3V, 2GH6, 3AOU, 4C4X, and 5F1J,<sup>31</sup> as these were the enzymes that gave results with a Tanimoto score  $\geq 0.7$  (Table S1 in Supporting Information). When their amino acid sequences were used in a search of the plant genomes, the highest score (410) was observed for 2GH6, which is a histone deacetylase. All the other enzymes had scores <296 (Supporting Information Table S2). Therefore, histone deacetylase seemed to be the target of the anilides in plants. Furthermore, as the amino acid sequences of enzymes transcribed from the plant genomes were very similar to that of 2GH6, it seemed reasonable to use the three-dimensional structure of this enzyme in a preliminary study with the aim of corroborating this initial result. Obviously, it would be better to use the three-dimensional structure of a histone deacetylase produced by plants, but unfortunately none is available.

Among the available three-dimensional structures of histone deacetylases, only 1ZZ0, 1ZZ1 and 1ZZ3<sup>53</sup> presented similarities to the amino acid sequence of 2GH6<sup>31</sup> that were >90%, had no missing amino acids in the three-dimensional structures of their binding sites, and were not mutants. Therefore, only these four histone deacetylases were employed in this study, which revealed affinities of compounds **4d**, **4g**, and **4h** for these enzymes that were statistically equivalent to those calculated for CF3, S17 and LLX, which are ligands, respectively, in the active sites of the crystalline structures of histone deacetylases 2GH6,<sup>37</sup> 2VCG,<sup>51</sup> and 3MAX.<sup>48</sup> For anilide **4i** and especially for **4e**, the affinities for the

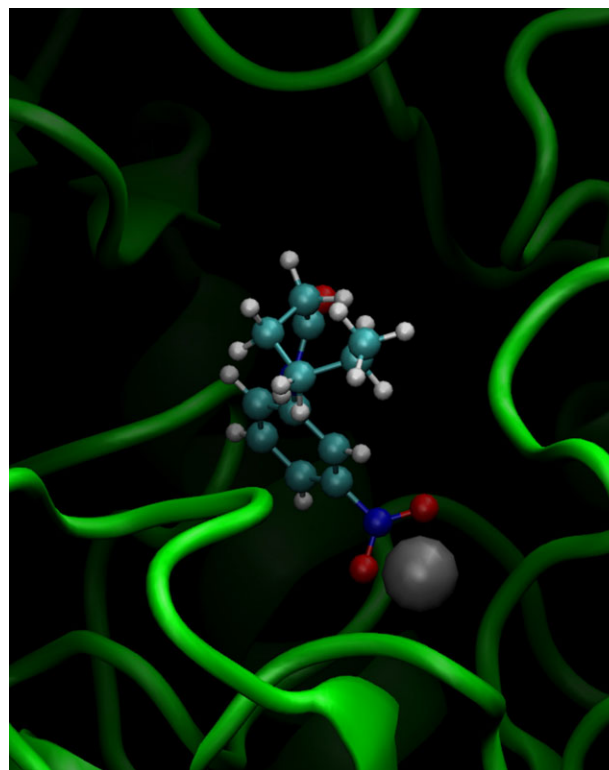


**Figure 4.** Expansion of the tridimensional structure of the active site of the enzyme histone deacetylase from *Alcaligenaceae* bacterium (code 1GH6 in the Protein Data Bank; <http://www.pdb.org>) containing *N*-(3-nitrophenyl)hexanamide (**4e**) in this active site. The ligand was docked to the enzyme using the computational program Autodock 4.2.6.<sup>47</sup> Enzyme and ligand were represented using NewCartoon and CPK format of VMD 1.9.2, respectively.<sup>29</sup>

enzymes were even greater. As the conformation of the 2GH6 site was adjusted to maximize the favorable interaction with CF3, these results indicate that the substances synthesized in the present work have good affinity for the enzyme.

This higher affinity of substance **4e** for the histone deacetylase is attributable to the interaction between the oxygen atoms of the nitro function and the  $\text{Zn}^{2+}$  ion (Figures 3 and 4). This interaction is in agreement with observations for CF3 (Figure 5), which also interacted with the same ion through oxygen atoms (Figures 6 and 7). In the case of substances **4d**, **4g**, **4h** and **4i**, interactions with the  $\text{Zn}^{2+}$  ion seem to be hampered by steric interactions between the enzyme and the groups bound to the oxygen atoms of these substances (Supporting Information Figs S45–S60).

Although data in the literature suggest that the action of amides against plants may be attributable to inhibition of photosystem II,<sup>54</sup> the results of the theoretical calculations carried out suggest that, for the substances synthesized in the present work, the enzymatic target is histone deacetylase, which has been exploited in the development of new herbicides by other research groups.<sup>55–59</sup>

## 4 CONCLUSIONS

Using one-pot methodologies, it was possible to obtain 18 anilides with good yields (36–98%), several of which were active against mono- and dicotyledonous plants. Among these, the most active were **2b**, **4d**, **4e**, **4g**, **4h** and **4i**, which showed greater inhibition than the commercial herbicide Dual Gold (*S*-metolachlor). In an *in silico* study, it was possible to verify that they act against the

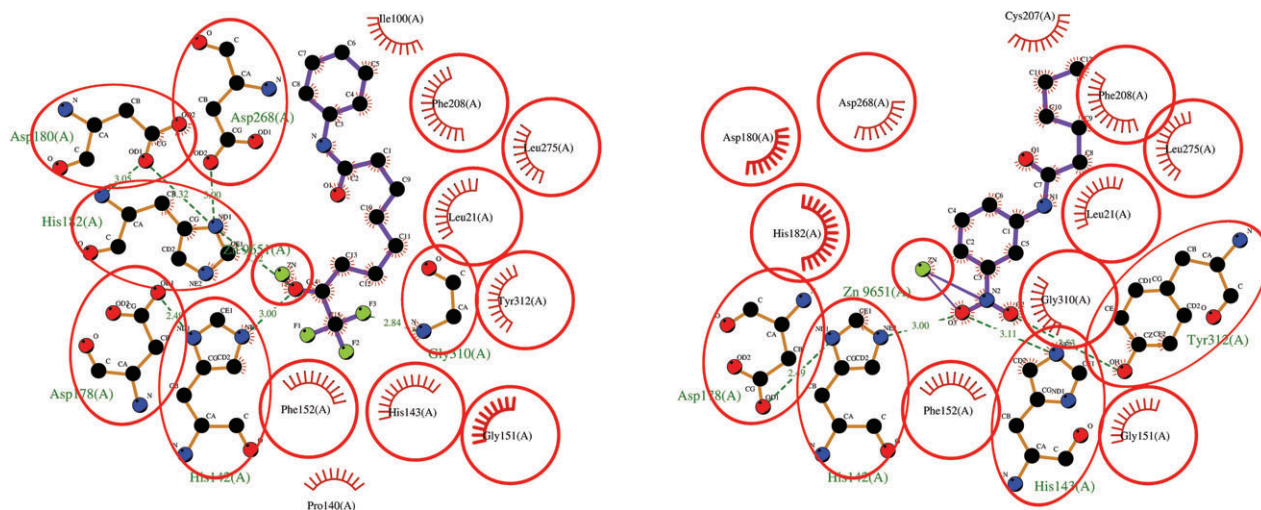


**Figure 5.** Two-dimensional representation of the interactions of 9,9,9-trifluoro-8-oxo-*N*-phenylnonanamide (CF3) and *N*-(3-nitrophenyl) hexanamide (**4e**) with the enzyme histone deacetylase from *Alcaligenaceae bacterium* (code 1GH6 in the Protein Data Bank; <http://www.pdb.org>). Ligands were docked to the active site of the enzyme with the software Autodock 4.2.6.<sup>47</sup> The image was generated in the software LigProt+1.4.5.<sup>60</sup>

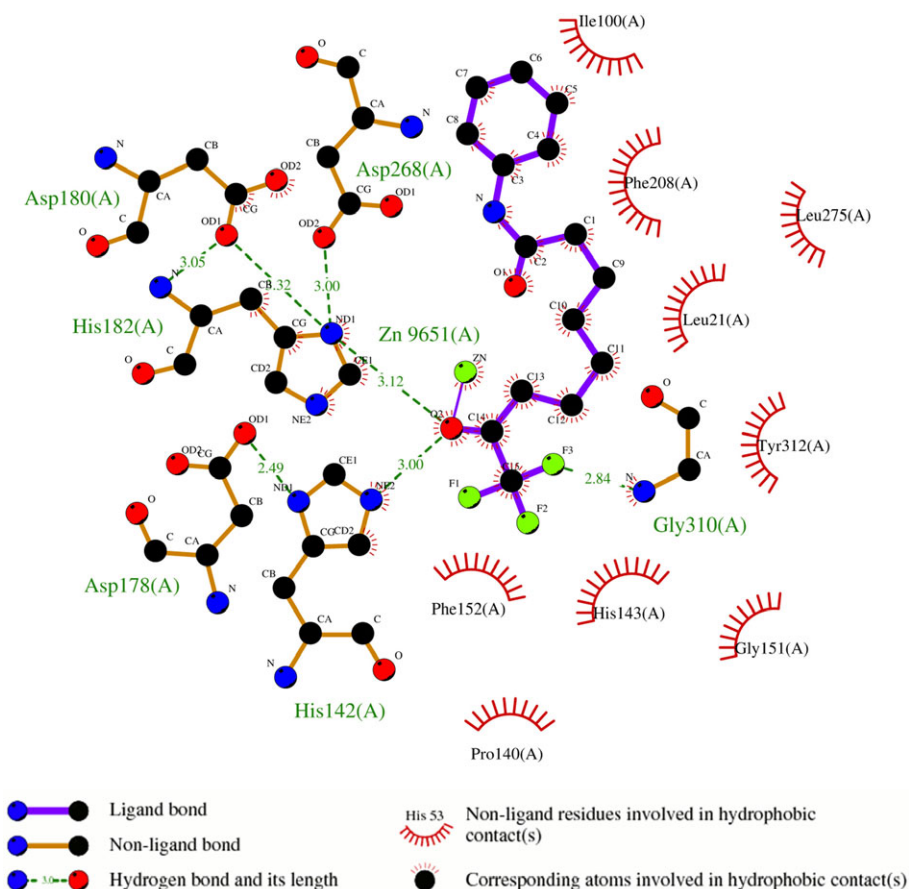


**Figure 6.** Two-dimensional representation of the interaction of 9,9,9-trifluoro-8-oxo-*N*-phenylnonanamide (CF3) with the enzyme histone deacetylase from *Alcaligenaceae bacterium* (code 1GH6 in the Protein Data Bank; <http://www.pdb.org>). The ligand was docked to the active site of the enzyme with the software Autodock 4.2.6.<sup>47</sup> The image was generated in the software LigProt+1.4.5.<sup>60</sup>



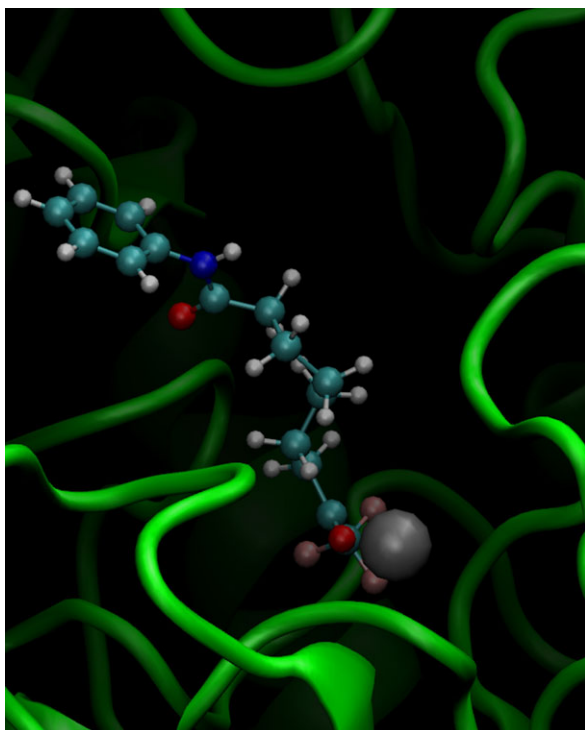


**Figure 7.** Expansion of the tridimensional structure of the active site of the enzyme histone deacetylase from *Alcaligenaceae* bacterium (code 1GH6 in the Protein Data Bank; <http://www.pdb.org>) containing 9,9,9-trifluoro-8-oxo-*N*-phenylnonanamide (CF3) in this active site. The ligand was docked to the enzyme using the computational program Autodock 4.2.6.<sup>47</sup> Enzyme and ligand were represented using NewCartoon and CPK format of VMD 1.9.2, respectively.<sup>29</sup>

plants by inhibiting the histone deacetylase enzyme, in which the affinity of the synthesized anilides is greater than that observed for some of its inhibitors. Therefore, it is concluded that the amides synthesized in this work, especially **2b**, **4d**, **4e**, **4g**, **4h** and **4i**, show great potential for use in the development of new herbicides.

## ACKNOWLEDGEMENTS

We thank the Brazilian Agencies CNPq, CAPES, RQ-MG, and FAPEMIG for financial support.

## SUPPORTING INFORMATION

Supporting information may be found in the online version of this article.

## REFERENCES

- Safdar ME, Tanveer A, Khaliq A and Riaz MA, Yield losses in maize (*Zea mays*) infested with parthenium weed (*Parthenium hysterophorus*L.). *Crop Protection* **70**:77–82 (2015).
- Teófilo TMS, Freitas FCL, Medeiros JF, Fernandes D, Grangeiro LC, Tomaz HVQ *et al.*, Eficiência no uso da água e interferência de plantas daninhas no meloeiro cultivado nos sistemas de plantio direto e convencional. *Planta Daninha* **30**:547–556 (2012).
- Resende GC, Alvarenga ES, Araújo TA, Campos JND and Picanço MC, Toxicity to *Diaphania hyalinata*, selectivity to non-target species and phytotoxicity of furanones and phthalide analogues. *Pest Manag Sci* **72**:1772–1777 (2016).
- Food and Agriculture Organization of the United Nations (FAOSTAT). OECD-FAO Agricultural outlook 2015–2024. [online]. Available: [https://doi.org/10.1787/agr\\_outlook-2015-en](https://doi.org/10.1787/agr_outlook-2015-en) [5 november 2016]

- Doležal M, Vičík R, Miletín M and Král'ová K, Synthesis and antimycobacterial, antifungal, and photosynthesis-inhibiting evaluation of some anilides of substituted pyrazine-2-carboxylic acids. *Chem Papers* **54**:245–248 (2000).
- Zitko J, Servusová B, Janoutová A, Paterová P, Mandíková J, Garaj V *et al.*, Synthesis and antimycobacterial evaluation of 5-alkylamino-*N*-phenylpyrazine-2-carboxamides. *Bioorg Med Chem* **23**:174–183 (2015).
- Buchenaeur H, Differences in light stability of some carboxylic acid anilide fungicides in relation to their applicability for seed and foliar treatment. *Pestic Sci* **6**:525–535 (1975).
- Nakagawa Y, Izumi K, Oikawa N, Kurozumi A, Iwamura H and Fujita T, Quantitative structure-activity relationships of benzoylphenylurea-larvicides. *Pestic Biochem Physiol* **4**:12–26 (1991).
- Doležal M, Vičík R, Miletín M and Král'ová K, Synthesis and antimycobacterial, antifungal, and photosynthesis-inhibiting evaluation of some anilides of substituted pyrazine-2-carboxylic acids. *Chem Papers* **54**:245–248 (2000).
- Tsikolia M, Bernier UR, Coy MR, Chalaire KC, Becnel JJ *et al.*, Insecticidal, repellent and fungicidal properties of novel trifluoromethylphenyl amides. *Pestic Biochem Physiol* **107**:138–147 (2013).
- Doležal M, Hartl J, Miletín M, Macháček M and Král'ová K, Synthesis and photosynthesis-inhibiting activity of some anilides of substituted pyrazine-2-carboxylic acids. *Chem Papers* **53**:126–130 (1999).
- Starmer GA, Mclean S and Thomas J, Analgesic potency and acute toxicity of substituted anilides and benzamides. *Toxicol Appl Pharmacol* **19**:20–28 (1971).
- Chiriac CI, Onciu M and Tanasa F, Synthesis of aromatic amides at room temperature using triphenyl phosphite-4-dimethylaminopyridine as reagent. *Des. Monomers Polym* **7**:331–335 (2004).
- Kanawi E, Scoy ARV, Budd R and Tjeerdema RS, Environmental fate and ecotoxicology of propanil: a review. *Toxicol Environ Chem* **98**:689–704 (2016).
- Paul S, Chakravarty A, Patra PK, Paul N, Sukul P and Mukherjee D, Microbe – Chloroacetanilide herbicide interaction across soil type. *Open Journal of Soil Science* **5**:87–99 (2015).
- Lee, WJ, Hoppin, JA, Blair A, Lubin JH, Dosemeci M *et al.*, Cancer incidence among pesticide applicators exposed to alachlor in the agricultural health study. *Am J Epidemiol* **159**:373–380 (2004).
- Mathias FT, Romano RM, Sleiman HK, Oliveira CA and Romano MA, Herbicide metolachlor causes changes in reproductive endocrinology of male wistar rats. *ISRN Toxicology* [online]. Available: <https://doi.org/10.5402/2012/130846> (2012).
- Miletín M, Hartl J and Macháček M, Synthesis of some anilides of 2-alkyl-4-pyridinecarboxylic acids and their photosynthesis-inhibiting activity. *Collect Czech Chem Commun* **62**:672–678 (1997).
- Král'ová K, Šeršeň F, Miletín M and Hartl J, Inhibition of photosynthetic electron transport by some anilides of 2-alkylpyridine-4-carboxylic acids in spinach chloroplasts. *Chem Papers* **52**:52–55 (1998).
- Busi R, Resistance to herbicides inhibiting the biosynthesis of very-long-chain-fatty acids. *Pest Manag Sci* **70**:1378–1384 (2014).
- Leelananda SP and Lindert S, Computational methods in drug discovery. *Beilstein J Org Chem* **12**:2694–2718 (2016).
- Abdolmaleki A, Ghasemi JB and Ghasemi F, Computer Aided Drug Design for Multi-Target Drug Design: SAR/QSAR, Molecular Docking and Pharmacophore Methods. *Current Drug Targets* **18**:556–575 (2017).
- Fu Y, Sun Y-N, Yi K-H, Li M-Q, Cao H-F, Li J-Z and Ye F, 3D Pharmacophore-Based Virtual Screening and Docking Approaches toward the Discovery of Novel HPPD Inhibitors. *Molecules* **22**:959–972 (2017).
- Alvarenga ES, Saliba WA and Milagres BG, Montagem de câmara com lâmpada de ultravioleta de baixo custo. *Quim Nova* **28**:927–929 (2005).
- Moraes FC, Alvarenga ES, Amorim KB, Demuner AJ and Pereira-Flores ME, Novel platensimycin derivatives with herbicidal activity. *Pest Manag Sci* **72**:580–584 (2016).
- Borgati TF, Alves RB, Teixeira RR, Freitas RP, Perdigão TG, Silva SF *et al.*, Synthesis and phytotoxic activity of 1,2,3-triazole derivatives. *J Braz Chem Soc* **24**:953–961 (2013).
- Tosco P, Balle T and Shiri F, Open3DALIGN: an opensource software aimed at unsupervised ligand alignment. *J Comput Aided Mol Des* **25**:777–783 (2011).
- Stewart JJP, MOPAC Version 15.286L. Stewart Computational Chemistry (2012).



- 29 Humphrey W, Dalke A and Schulten KJ, VMD: Visual Molecular Dynamics. *J Mol Graphics* **14**:33–38 (1996).
- 30 Feng Z, Chen L, Maddula H, Akcan O, Oughtred R, Berman HM *et al.*, Ligand Depot: a data warehouse for ligands bound to macromolecules. *Bioinformatics* **20**:2153–2155 (2004).
- 31 Berman HM, Westbrook J, Feng Z, Gilliland G, Bhat TN, Weissig H *et al.*, The Protein Data Bank. *Nucleic Acids Res.* **28**:235–242 (2000).
- 32 O'Boyle NM, Banck M, James CA, Morley C, Vandermeersch T and Hutchison GR, "Open Babel: An open chemical toolbox". *J Cheminf* **3**:33 (2011).
- 33 Taminau J, Thijs G and De Winter H, Pharao: pharmacophore alignment and optimization. *J Mol Graph Model* **27**:161–169 (2008).
- 34 Peón A, Naulaerts S and Ballester PJ, Predicting the reliability of drug-target interaction predictions with maximum coverage of target space. *Scientific Reports* **7**:3820 (2017).
- 35 Wouters J, Fonze E, Vermeire M, Frère J-M and Charlier P, Crystal structure of Enterobacter cloacae 908R class C beta-lactamase bound to iodo-acetamido-phenyl boronic acid, a transition-state analogue. *Cell Mol Life Sci* **60**:1764–1773 (2003).
- 36 Hori T, Yokomizo T, Ago H, Sugahara M, Ueno G, Yamamoto M *et al.*, Structural basis of leukotriene B<sub>4</sub> 12-hydroxydehydrogenase/15-Oxo-prostaglandin 13-reductase catalytic mechanism and a possible Src homology 3 domain binding loop. *J Biol Chem* **279**:22615–22623 (2004).
- 37 Nielsen TK, Hildmann C, Riester D, Wegener D, Schwienhorst A and Ficner R, Complex structure of a bacterial class 2 histone deacetylase homologue with a trifluoromethylketone inhibitor. *Acta Crystallogr Sect F* **63**:270–273 (2007).
- 38 Mizutani K, Yamamoto M, Suzuki K, Yamato I, Kakinuma Y, Shirouzu M *et al.*, Structure of the rotor ring modified with *N,N'*-dicyclohexylcarbodiimide of the Na<sup>+</sup>-transporting vacuolar ATPase. *Proc Natl Acad Sci USA* **108**:13474–13479 (2011).
- 39 Pilger J, Mazur A, Monecke P, Schreuder H, Elshorst B, Bartoschek S *et al.*, A Combination of spin diffusion methods for the determination of protein-ligand complex structural ensembles. *Angew Chem Int Ed Engl* **54**:6511–6515 (2015).
- 40 Nikiforov PO, Surade S, Blaszczyk M, Delorme V, Brodin P, Baulard AR *et al.*, A fragment merging approach towards the development of small molecule inhibitors of *Mycobacterium tuberculosis* EthR for use as ethionamide boosters. *Org Biomol Chem* **14**:2318–2326 (2016).
- 41 Altschul SF, Madden TL, Schäffer AA, Zhang J, Zhang Z, Miller W *et al.*, Gapped BLAST and PSI-BLAST: a new generation of protein database search programs. *Nucleic Acids Res* **25**:3389–3402 (1997).
- 42 Schäffer AA, Aravind L, Madden TL, Shavirin S, Spouge JL, Wolf YI *et al.*, Improving the accuracy of PSI-BLAST protein database searches with composition-based statistics and other refinements. *Nucleic Acids Res.* **29**:2994–3005 (2001).
- 43 Boratyn GM, Schäffer AA, Agarwala R, Altschul SF, Lipman DJ and Madden TL, Domain enhanced lookup time accelerated BLAST. *Biol Direct* **7**:12 (2012).
- 44 Okonechnikov K, Golosova O and Fursov M, Unipro UGENE: a unified bioinformatics toolkit. *Bioinformatics* **28**:1166–1167 (2012).
- 45 Sievers F, Wilm A, Dineen DG, Gibson TJ, Karplus K, Li W *et al.*, Fast, scalable generation of high-quality protein multiple sequence alignments using Clustal Omega. *Mol Syst Biol* **7**:539 (2011).
- 46 Martínez L, Andreani R and Martínez JM, Convergent algorithms for protein structural alignment. *BMC Bioinformatics* **8**:306 (2007).
- 47 Morris GM, Huey R, Lindstrom W, Sanner MF, Belew RK, Goodsell DS *et al.*, Autodock4 and AutoDockTools4: automated docking with selective receptor flexibility. *J Comput Chem* **30**:2785–2791 (2009).
- 48 Bressi JC, Jennings AJ, Skene R, Wu Y, Melkus R, De Jong R *et al.*, Exploration of the HDAC2 foot pocket: Synthesis and SAR of substituted *N*-(2-aminophenyl)benzamides. *Bioorg Med Chem Lett* **20**:3142–3145 (2010).
- 49 Dowling DP, Gattis SG, Fierke CA and Christianson DW, Structures of metal-substituted human histone deacetylase provide mechanistic inferences on biological function. *Biochemistry* **49**:5048–5056 (2010).
- 50 Whitehead L, Dobler MR, Radetich B, Zhu Y, Atadja PW, Claiborne T *et al.*, Human HDAC isoform selectivity achieved via exploitation of the acetate release channel with structurally unique small molecule inhibitors. *Bioorg Med Chem* **19**:4626–4634 (2011).
- 51 Schäfer S, Saunders L, Eliseeva E, Veleno A, Jung M, Schwienhorst A *et al.*, Phenylalanine-containing hydroxamic acids as selective inhibitors of class IIb histone deacetylases (Hdacs). *Bioorg Med Chem* **16**:2011–2033 (2008).
- 52 Ferreira DF, Sisvar: a computer statistical analysis system. *Ciência e Agrotecnologia (UFPA)* **35**:1039–1042 (2011).
- 53 Nielsen TK, Hildmann C, Dickmanns A, Schwienhorst A and Ficner R, Crystal structure of a bacterial class 2 histone deacetylase homologue. *J Mol Biol* **354**:107–120 (2005).
- 54 Lewis RJ, Camilleri P, Kirby AJ, Marby CA, Slawin AA and Williams D J, Structure-activity studies on amides inhibiting photosystem II. *J Chem Soc, Perkin Trans 2*:1625–1630 (1991).
- 55 Hollender C and Liu Z, Histone deacetylase genes in *Arabidopsis* development. *J Integr Plant Biol* **50**:875–885 (2008).
- 56 Gregoret IV, Lee YM and Goodson HV, Molecular evolution of the histone deacetylase family: functional implications of phylogenetic analysis. *J Mol Biol* **338**:17–31 (2004).
- 57 Liu X, Yang S, Zhao M, Luo M, Yu C-W, Chen C-Y *et al.*, Transcriptional repression by histone deacetylases in plants. *Mol Plant* **7**:764–772 (2014).
- 58 Venturelli S, Belz RG, Kämper A, Berger A, Horn K, Wegner A *et al.*, Plants release precursors of histone deacetylase inhibitors to suppress growth of competitors. *The Plant Cell* **27**:3175–3189 (2015).
- 59 Ma X, Lv S, Zhang C and Ping Y, Histone deacetylases and their functions in plants. *Plant Cell Rep* **32**:465–478 (2013).
- 60 Wallace AC, Laskowski RA and Thornton JM, LIGPLOT: a program to generate schematic diagrams of protein-ligand interactions. *Protein Eng* **8**:127–134 (1995).